DOI 10.59887/2073-6673.2024.17(3)-6

UDC 551.463.5

© *D. I. Glukhovets**[1,2], *S. V. Sheberstov*[1], 2024

© Translated from Russian: *E. S. Kochetkova*, 2024

[1]Shirshov Institute of Oceanology, Russian Academy of Sciences, 117997, Nakhimovsky pr., 36, Moscow, Russia
[2]Moscow Institute of Physics and Technology (National Research University), 141701, Institutskiy per., 9, Dolgoprudny, Moscow Region, Russia
*glukhovets@ocean.ru

INFLUENCE OF PHYTOPLANKTON ON OCEAN ALBEDO

Received 02.04.2024, Revised 10.09.2024, Accepted 18.09.2024

Abstract

Using numerical methods for solving the radiation transfer equation, ocean albedo values were calculated for a set of bio-optical characteristics corresponding to situations with different chlorophyll concentrations (1 μg/L and 10 μg/L) and the case of intense coccolithophore bloom (8–12 million cells/L). Calculations were carried out in the spectral range of 280–2800 nm for cases of cloudless sky at various wind speeds and atmospheric transmission. It has been shown that for Case 1 waters, a change in chlorophyll concentration from 1 to 10 μg/L does not lead to changes in albedo. In the case of intense coccolithophore blooms, the ocean albedo can increase more than threefold. Calculation of average monthly albedo values for selected points in the Barents and Black seas showed that the presence of intense coccolithophore blooms significantly increases average monthly albedo values. The calculation of the values of radiation absorbed in the seawater column depending on the time of day, carried out for these points, demonstrated that the presence of blooms significantly reduces the values of absorbed radiation. It is shown that the contribution to the albedo of radiation emerging from water used in the state-of-the-art NEMO circulation numerical ocean model, amounting to 0.005±0.0005, corresponds only to Case 1 waters. Intense coccolithophore blooms can increase this contribution by more than 14 times. A simple formula is proposed for correcting albedo values taking into account the influence of bio-optical characteristics.

Keywords: ocean albedo, solar radiation absorption, hydrooptical modeling, chlorophyll, coccolithophore bloom, Black Sea, Barents Sea

УДК 551.463.5

© *Д. И. Глуховец**[1, 2], *С. В. Шеберстов*[1], 2024

© Перевод с русского: *Е. С. Кочеткова*, 2024

[1]Институт океанологии им. П.П. Ширшова, РАН, 117997, Нахимовский пр., д. 36, Москва
[2]Московский физико-технический институт (национальный исследовательский университет), 141701, Институтский пер., 9, г. Долгопрудный, Московская область
*glukhovets@ocean.ru

ВЛИЯНИЕ ФИТОПЛАНКТОНА НА АЛЬБЕДО ОКЕАНА

Статья поступила в редакцию 02.04.2024, после доработки 10.09.2024, принята в печать 18.09.2024

Аннотация

С использованием численных методов решения уравнения переноса излучения рассчитаны значения альбедо океана для набора биооптических характеристик, соответствующих ситуациям с различной концентрацией хлорофилла (1 мкг/л и 10 мкг/л) и случаю интенсивного кокколитофоридного цветения (8–12 млн кл./л). Расчеты проводились в спектральном интервале 280–2800 нм для случаев безоблачного неба при различных скоростях приводного ветра и пропускания атмосферы. Показано, что для вод первого оптического типа изменение концентрации хлорофилла от 1 до 10 мкг/л не приводит к изменениям альбедо. В случае интенсивного кокколитофоридного цветения альбедо океана может увеличиваться более, чем в три раза. Расчет среднемесячных значений альбедо для выбранных точек в Баренцевом и Черном морях показал, что наличие интенсивного кокколитофоридного цветения существенно увеличивает среднемесячные значения альбедо. Выполненный для

Ссылка для цитирования: *Глуховец Д.И.*, *Шеберстов С.В.* Влияние фитопланктона на альбедо океана // Фундаментальная и прикладная гидрофизика. 2024. Т. 17, № 3. С. 73–83. doi:10.59887/2073-6673.2024.17(3)-6
For citation: Glukhovets D.I., Sheberstov S.V. Influence of Phytoplankton on Ocean Albedo. *Fundamental and Applied Hydrophysics*. 2024;17(3):73–83. doi:10.59887/2073-6673.2024.17(3)-6

этих точек расчет величин поглощенного в толще морской воды излучения в зависимости от времени суток продемонстрировал, что наличие цветения существенно уменьшает величины поглощенной радиации. Показано, что принятый в современной циркуляционной модели NEMO вклад в альбедо выходящего из воды излучения, составляющий 0,005 ± 0,0005, соответствует только водам первого оптического типа. Интенсивное цветение кокколитофорид может привести к увеличению этого вклада более чем в 14 раз. Предложена простая формула для коррекции значений альбедо с учетом влияния биооптических характеристик.

Ключевые слова: альбедо океана, поглощение солнечной радиации, гидрооптическое моделирование, хлорофилл, кокколитофоридное цветение, Черное море, Баренцево море

1. Introduction

In oceanography, the impact of the hydro-optical characteristics of seawater on ocean albedo has traditionally been insufficiently addressed. Notably, in the monograph [1] dedicated to the radiation regime of the oceans, parameters such as the transparency and color of seawater are mentioned only in the context of wave effects on albedo values. However, albedo is one of the most critical parameters for calculating the Earth's radiative balance [2, 3], and its variations significantly influence the variability of the Earth's climate system [4].

In several studies [5–7], researchers have focused on the albedo of the atmosphere-ocean system, commonly referred to as "Top of the Atmosphere Albedo"[1]. This focus is driven by the fact that planetary albedo is, on average, determined by approximately 88 % of the radiation reflected by the atmosphere [8]. In this context, the contribution of the underlying surface is often negligible, which helps to explain the limited attention given by researchers to the role of hydro-optical characteristics. However, for certain issues — particularly the assessment of the amount of solar radiation absorbed in the seawater column — accurate values of ocean albedo are essential [9].

In the current NEMO circulation model [10], the results of study [11] are used, in which the contribution of outgoing radiation from the water is fixed. It is assumed that, for the wavelength range of 280–2800 nm, this contribution amounts to 0.005 ± 0.0005. This value is considered representative of most waters in the World Ocean. A detailed analysis of the main factors influencing ocean albedo — such as the solar zenith angle, wind speed, atmospheric transmittance (including gasses, aerosols, and clouds), and chlorophyll concentration — was conducted in study [12]. Based on numerical solutions to the radiative transfer equation, validated by direct albedo measurements from an oceanographic platform located 25 km off Virginia Beach (Atlantic Coast, USA), tables were compiled for each of the investigated factors. A relatively recent article [13] proposed a calculation scheme for ocean albedo that incorporates the aforementioned factors, presenting results from its integration into the RRTMG_SW atmospheric model developed by the U.S. Department of Energy. Comparisons of the simulation results with data from various field experiments demonstrated good agreement. It is important to note that both studies mentioned above assumed Case 1 waters, where the optical characteristics of seawater are described solely by chlorophyll concentration. Clearly, this approach can lead to errors in many regions of the World Ocean, where the correlation between chlorophyll concentration and hydro-optical characteristics is absent, particularly in areas affected by river runoff and mass blooms of coccolithophores [14]. Study [15] showed the significant impact of coccolithophore blooms on ocean albedo, although it was limited to a narrow spectral range and did not account for the effects of wind and atmospheric transmittance. The present work addresses these shortcomings by demonstrating the variability of ocean albedo driven by hydro-optical characteristics of natural waters with various phytoplankton communities in the relevant spectral range of solar radiation (280–2800 nm) reaching the Earth's surface, under different wind speeds and aerosol optical thicknesses. Examples of intense coccolithophore blooms in the Black and Barents seas are examined, with hydro-optical and biological characteristics obtained during expeditions conducted by the P.P. Shirshov Institute of Oceanology of the Russian Academy of Sciences.

2. Methods

To calculate ocean albedo, numerical methods for solving the radiative transfer equation in the atmosphere-ocean system were employed, primarily the matrix operator method [16], which is based on the application of recursive formulas to the reflection (R) and transmission (T) operators for homogeneous plane-parallel layers. In our study, we applied a modified version of this method, which is described in detail in [17].

1 https://ceres.larc.nasa.gov/resources/images/ (date of access: 25.03.2024)

For the atmosphere, we employ a three-layer model: the upper layer is a non-scattering absorbing layer of ozone (300 DU), the second layer represents a Rayleigh atmosphere, and the third layer consists of aerosols characterized by the Gordon and Castaño model [18] with an optical thickness of $\tau_a(\lambda) = \tau_a(869)\left(\frac{869}{\lambda}\right)^{1.6}$ and $\tau_a(869) = 0.2$. In the infrared region of the spectrum, the absorption of water vapor significantly impacts the atmospheric transmittance. We applied HITRAN data for the spectral dependence of absorption coefficients for water vapor and ozone, which are available on the website [19] of the V.E. Zuev Institute of Atmospheric Optics, Siberian Branch of the Russian Academy of Sciences.

The surface is considered as a separate layer. The formulas for a smooth surface can be found in work [17], while the results for a wind-ruffled surface were obtained from [20].

To estimate the primary hydro-optical characteristics of the water layers, a one-parameter Case I new model [21, 22] was used, in which all optical characteristics are uniquely defined by chlorophyll concentration (*Chl*). In the case of coccolithophore blooms, scattering was described using the two-parameter Kopelevich's model [23]. For the calculation of absorption and scattering by pure water in the spectral range of 280–2800 nm, data from [24] were used.

The discrete ordinate method (DISORT) [25] was employed to compute the reflection and transmission operators for individual layers.

Additionally, the HydroLight software [21] was used for the calculations. Case 1 new and Case 2 new models were applied under clear sky conditions and in the absence of wind. Effects of inelastic scattering were not modeled.

In modeling coccolithophore blooms, typical values of hydro-optical characteristics obtained from shipboard expeditions in the Barents and Black seas [26] were used. The ratio of the backward scattering coefficient to the total scattering coefficient (b_b/b) was assumed to be 0.02, consistent with the findings in study [27]. The seawater beam attenuation coefficient at the wavelength of 530 nm, $c(530)$, was set to 3 m^{-1}, which corresponds to an intense bloom with coccolithophore concentrations of 8–12 million cells/L [26]. The spectral dependence of the scattering coefficient was taken as follows:

$$b(\lambda) = c(\lambda) - a(\lambda) = c(530)\frac{530}{\lambda} - a(\lambda). \quad (1)$$

The spectral albedo values were calculated using the formula:

$$A(\lambda) = \frac{E_u(\lambda)}{E_d(\lambda)}, \quad (2)$$

where $E_d(\lambda)$ is the spectral irradiance above the water surface created by the downward radiation flux, and $E_u(\lambda)$ is the spectral irradiance above the water surface created by the upward radiation flux.

The average albedo values for the range of 280–2800 nm were calculated using the formula:

$$A(\theta_0) = \frac{\int_{280}^{2800} E_u(\lambda,\theta_0)d\lambda}{\int_{280}^{2800} E_d(\lambda,\theta_0)d\lambda}, \quad (3)$$

where θ_0 is the solar zenith angle.

Atmospheric transmittance was determined as:

$$T(\theta_0) = \frac{\int_{280}^{2800} E_d(\lambda,\theta_0)d\lambda}{\cos(\theta_0)\int_{280}^{2800} F_0(\lambda)d\lambda}, \quad (4)$$

where $F_0(\lambda)$ is the solar constant.

The calculation of daily average albedo values was conducted according to the expression:

$$\overline{A} = \frac{\overline{E}_u}{\overline{E}_d} = \frac{\sum_i \int_{280}^{2800} A(\lambda, \theta_0^i) E_u(\lambda, \theta_0^i) d\lambda}{\sum_i \int_{280}^{2800} E_d(\lambda, \theta_0^i) d\lambda}, \quad (5)$$

where the index i denotes the discrete temporal values included in the expression. In the calculations of daily average albedo, hourly values of the solar zenith angle were used, computed for selected points in the Barents and Black seas. The other variables were interpolated based on the data from the conducted calculations.

3. Results

Spectral values of the sea remote sensing reflectance $R_{rs}(\lambda)$ and albedo $A(\lambda)$, obtained using HydroLight for various solar zenith angles θ_0 in the visible range of the spectrum — where the influence of hydro-optical characteristics related to variations in phytoplankton parameters in seawater is most pronounced — are presented in Fig. 1. The calculations used the Case 1 new approximation with two chlorophyll concentrations of 1 and 10 μg/L. Notably, the values of $R_{rs}(\lambda)$ exhibit low variability with changes in θ_0. This stability is attributed to the use of normalized water-leaving radiance in the calculation of this quantity. This resilience to variations in lighting conditions supports the widespread use of $R_{rs}(\lambda)$ in remote sensing. In contrast, ocean albedo values exhibit significantly greater variability with changes in the solar zenith angle. This variability arises due to the increase in the water surface reflection coefficient with increasing angle of incidence, according to Fresnel's law.

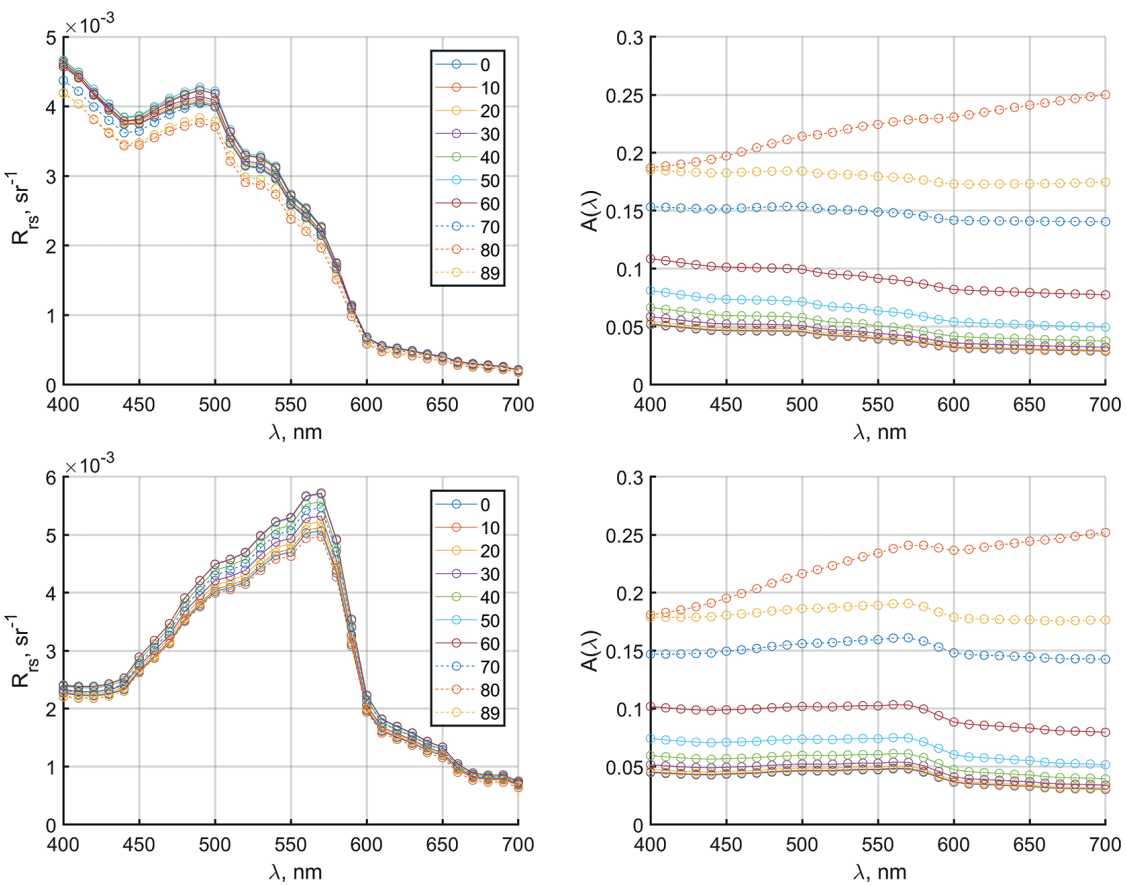

Fig. 1. Spectral values of the sea remote sensing reflectance (left column) and albedo (right column), obtained using HydroLight for various solar zenith angles θ_0. Case 1 model, with Chl = 1 μg/L (top row) and Chl = 10 μg/L (bottom row)

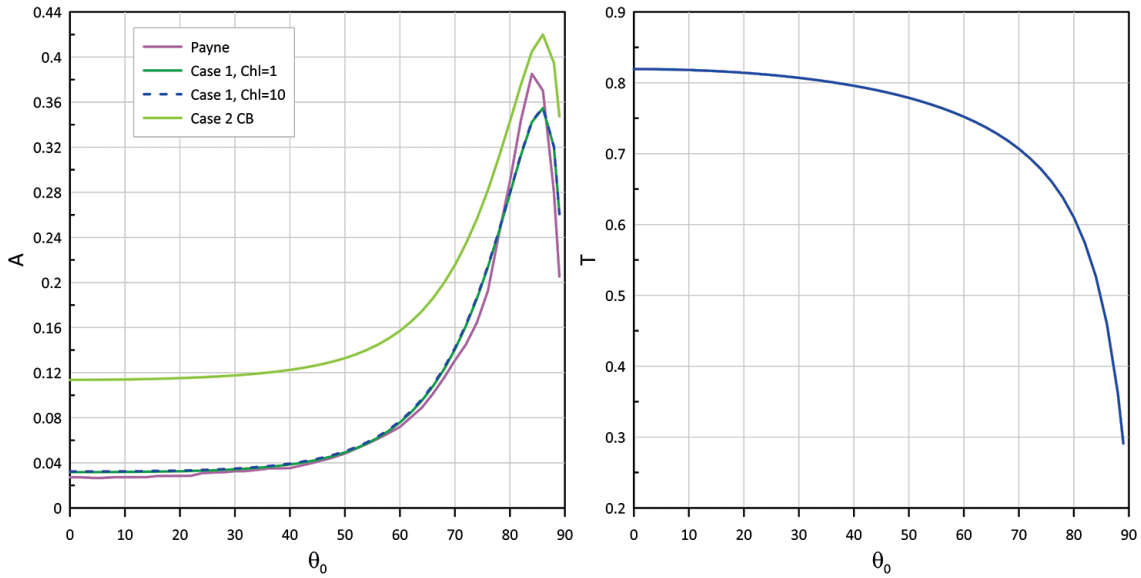

Fig. 2. Left: Averaged albedo values in the range of 280–2800 nm, obtained using DISORT for various scenarios: *Chl* = 1 μg/L; *Chl*=10 μg/L; coccolithophore bloom, c(530) = 3 m^{-1}. For comparison, data from work [11] are presented. Right: Atmospheric transmittance dependence for various solar zenith angles θ_0

The results of the calculations performed for Case 1 waters indicate that the contribution of radiation reflected from the water surface to $A(\lambda)$ is substantially greater than the contribution of radiation emerging from the seawater column, even at a relatively high chlorophyll concentration of 10 μg/L, which is typical for the waters of the World Ocean. This concentration primarily influences the shapes of the $A(\lambda)$ spectra, resulting in minimal changes to their average levels (Fig. 1, right).

Similar calculations across the full spectral range of 280–2800 nm were conducted using software developed on the basis of the discrete ordinate method (DISORT) [17]. The averaged albedo values obtained for various situations in this spectral interval are shown on the left side of Fig. 2. In addition to the aforementioned examples of Case 1 waters, results obtained for the case of an intense coccolithophore bloom (Case 2) are presented. For Case 1 waters, variations in *Chl* from 1 to 10 μg/L do not lead to changes in albedo *A*. This is related to the combined changes in absorption and scattering coefficients. In the case of a coccolithophore bloom, however, ocean albedo can increase by more than threefold. For comparison, albedo values from work [11] have been added to the graph. In this analysis, in addition to the solar zenith angle, variations in atmospheric transmittance — also calculated during the modeling —were taken into account (Fig. 2, right). The results indicate that the widely accepted model does not account for the significant increase in the scattered radiation emerging from the water, which is typical for coccolithophore blooms, and slightly overestimates the values of $A(\theta_0)$ at solar zenith angles greater than 80° for Case 1 waters.

Table 1 presents the average monthly ocean albedo values for selected points in the Barents Sea (70° N, 40° E) and the Black Sea (44.5° N, 38° E — Black Sea test site of the IO RAS) during months of regular coccolithophore blooms, with the results generated under the assumption of Case 2 waters. These values were obtained by averaging daily albedo values, calculated according to equation 5 for all days of the month.

Table 1

Monthly average values of *A* in the 280–2800 nm range for the period of coccolithophore bloom in cases with (CB) and without its presence, as well as data from study [11]

	Case 1, *Chl* = 1 μg/L	Case 2, CB	Payne, 1972 [11]
Barents Sea, August	0.106	0.156	0.09
Black sea, June	0.054	0.108	0.06

For comparison, calculations were also made assuming no blooms-representing Case 1 waters. The albedo values for waters free from coccolithophore blooms correspond well with classic results [11], showing a discrepancy of about 15 % for the Barents Sea and around 10 % for the Black Sea. The presence of intense coccolithophore blooms significantly increases the average monthly albedo values: by 1.5 times in the Barents Sea and by twofold in the Black Sea. The difference in the impact of blooms is explained by the larger solar zenith angles at higher latitudes, which reduces the contribution of radiation emerging from the water to the total albedo.

4. Discussion

Fig. 3 shows the contributions of solar radiation absorbed within the water column at different times of day, both during intense coccolithophore blooms and in their absence, for a location at the Black Sea polygon of the IO RAS. The significant differences are due to the considerable variability in albedo (Fig. 2). Notably, the contribution of dawn and dusk hours to total absorption is 0.32 % (0.4 % for the Barents Sea). This is explained by the fact that light conditions have a greater impact on the energy absorbed in the water column than albedo. During dawn and dusk, the solar zenith angle exceeds 80°. As a result, the inaccuracies in albedo estimates reported in study [11], particularly beyond 80°, do not cause substantial errors in calculating the daily absorbed radiation within the water column. Similar results were found for the Barents Sea.

The dependence of ocean albedo on the solar zenith angle at various wind speeds for a $Chl = 1$ μg/L is shown in Fig. 4. At small solar zenith angles, albedo values are slightly higher for rough sea surfaces in comparison to calm conditions. It is the result of better reflection of incident rays from inclined surfaces than horizontal ones. At larger zenith angles, surface roughness reduces albedo, as the rays are more likely to penetrate the water column. As wind speed increases, albedo decreases more sharply at zenith angles greater than 60°.

As previously demonstrated, ocean albedo in the visible spectrum can be significantly influenced by the hydro-optical properties of seawater, which are related to the variability in the structural and quantitative characteristics of phytoplankton. Although the visible range constitutes only a portion of the spectrum, the variability

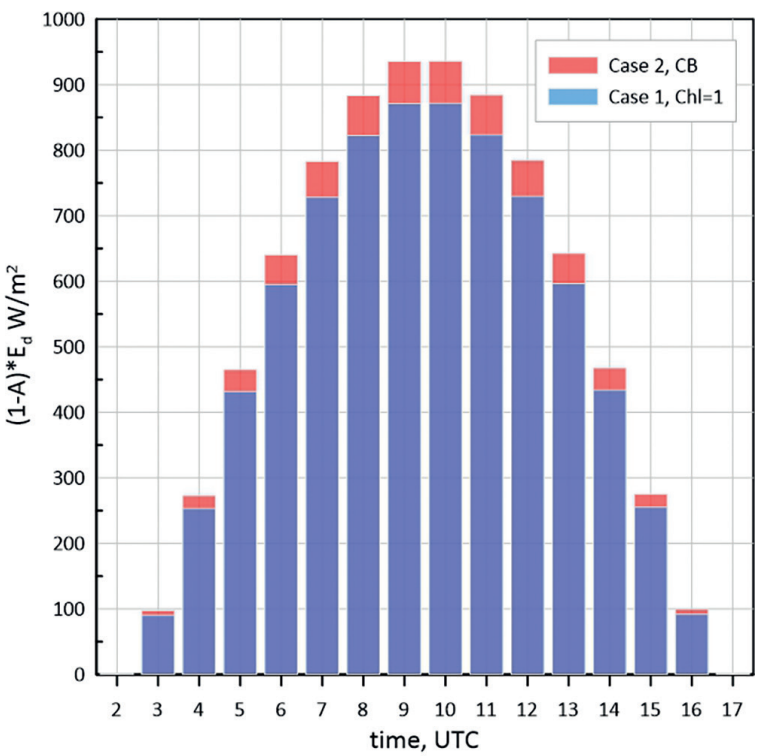

Fig. 3. The relationship between the amounts of radiation absorbed in the water column and the time of day, during and without intense coccolithophore blooms, Black Sea, June 15

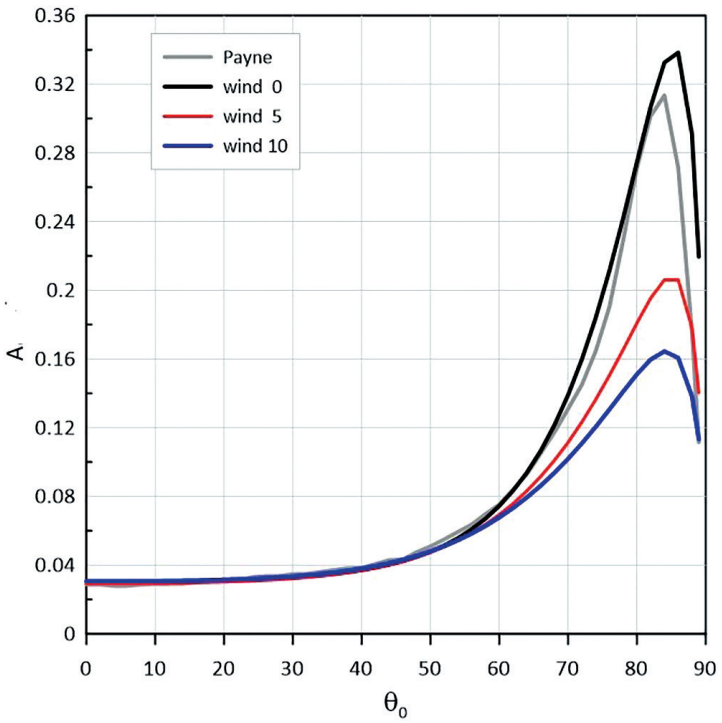

Fig. 4. The relationship between ocean albedo and solar zenith angle at different wind speeds

of bio-optical properties observed within it affects the values of A across the entire range. To verify the assertion made in study [11] that the contribution of radiation emitted from the water surface to albedo (A_w) is 0.005 ± ± 0.0005, we will limit our calculations to a narrower spectral range. Since radiation in the near-infrared is largely absorbed by seawater and does not emerge from the water column, and because radiation with wavelengths shorter than 300 nm hardly penetrates the Earth's ozone layer, it is sufficient to examine the range of 300–1000 nm, outside of which hydro-optical properties do not influence albedo. The following expression is used to calculate the fraction of albedo formed by the water column:

$$A_w = \pi \frac{\int_{300}^{1000} R_{rs}(\lambda) E_d(\lambda) d\lambda}{\int_{300}^{1000} E_d(\lambda) d\lambda}. \quad (6)$$

For the Case I waters with a chlorophyll concentration of 1 μg/L, the value of $A_w = 0.0054$, which fully aligns with the data from study [11]. However, during intense coccolithophore blooms, this value increases to $A_w = 0.077$, more than 14 times higher than the corresponding value observed in the absence of blooms. This component of albedo accounts for the discrepancies shown in Table 1. Such a difference is consistent with the results of study [27], where the authors modeled the impact of coccolithophore blooms on albedo by specifying values for calcite concentration. For model values of chlorophyll at 0.75 μg/L, a solar zenith angle θ_0 of 45°, wind speed of 5 m/s, and 25 % cloud cover, the fraction of radiation emitted from the water surface increases from 0.4 % to 5.2 % with the addition of 300 mg of $CaCO_3$–C m^{-3}.

The obtained results highlight the importance of considering the hydro-optical properties associated with the variability in the structural and quantitative characteristics of phytoplankton when calculating ocean albedo. The necessary adjustment can be made using Equation (6) based on the standard product from ocean color scanners, specifically the remote sensing reflectance $R_{rs}(\lambda)$. This consideration is crucial because coccolithophore blooms regularly cover significant areas of the global ocean and can persist for approximately one month [14].

Fig. 5 illustrates the relationship between ocean albedo and atmospheric transmittance as a function of the aerosol optical thickness for the aerosol optical properties model presented in Section 2. As shown, an

increase in optical thickness from 0.05 to 0.3 results in a smoothing of the angular dependence of albedo and an insignificant (<0.5 %) change in the daily average albedo. However, the change in the daily absorbed radiation within the water column is approximately 5 %.

Future developments of this work should take cloud cover into account. It is crucial to select the most accurate source of data regarding the average density and optical properties of clouds. This selection appears to be a challenging task. Study [28] demonstrates that even the annual variation in hemispherically averaged cloud cover over the ocean, determined from various satellite data, observations, and reanalyses, can differ by nearly a factor of two. A more straightforward approach is to analyze the impact of differences in the bio-optical properties of seawater on the albedo of a clear sky during the day ("Top of the Atmosphere Clear-sky Albedo"[2]), where the contribution of clouds is excluded, but the influence of the atmosphere is considered.

Furthermore, a promising direction for future research is the detailed examination of areas influenced by river runoff. An example of such a water body is the Kara Sea, where a significant area is affected by this phenomenon [29]. Two opposing factors are expected to influence ocean albedo: scattering of radiation by suspended particles tends to increase albedo values, while absorption by colored dissolved organic matter tends to decrease them. An illustration of the effects of these factors can be found in Table 1 of study [30], which presents albedo values for the waters of various rivers.

5. Conclusion

Using a numerical solution to the radiative transfer equation within the atmosphere-wind-roughened ocean system, this study demonstrates how phytoplankton influences the variability of ocean albedo. Calculations were conducted across the spectral range of 280–2800 nm, which corresponds to the solar radiation that reaches the Earth's surface, under clear sky conditions, varying wind speeds, and atmospheric transmittance. While changes in chlorophyll concentration from 1 to 10 μg/L have little impact on A, intense coccolithophore blooms can lead to more than a threefold increase in ocean albedo. This phenomenon is not accounted for in commonly used ocean albedo data sources [11]. It is shown that inaccuracies in determining A at high solar zenith angles do not lead to substantial errors in calculating the daily absorbed radiation within the water column during the summer months in both the Black Sea and the Barents Sea. The obtained results underscore the importance of

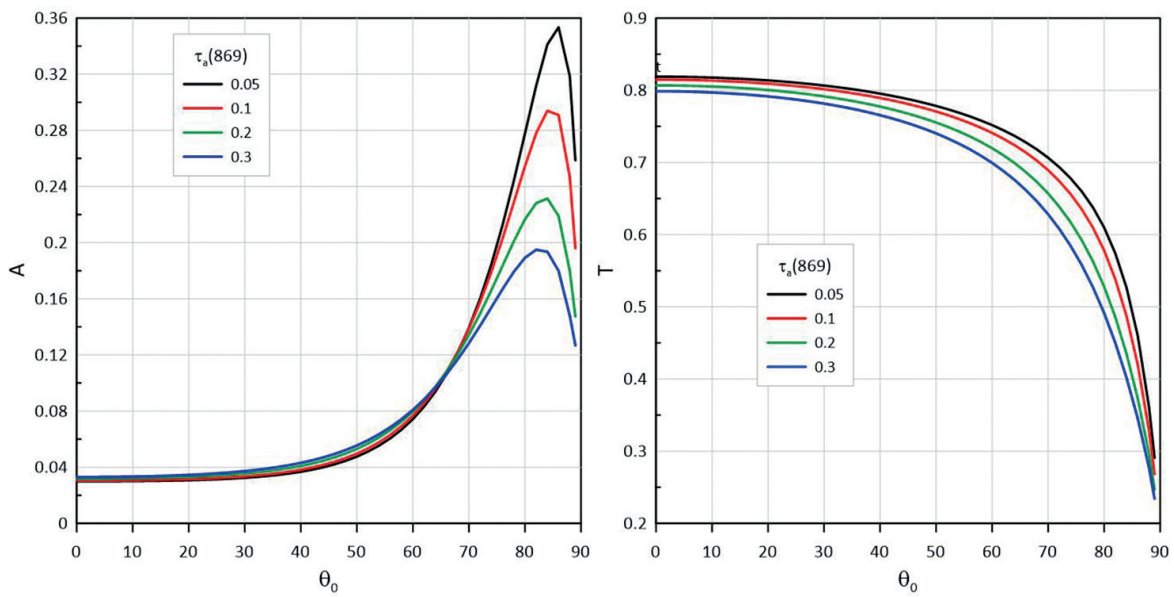

Fig. 5. The relationship between ocean albedo (left) and atmospheric transmittance (right) as a function of solar zenith angle at different values of aerosol optical thickness

[2] https://ceres.larc.nasa.gov/resources/images/ (date of accesss: 25.03.2024)

considering bio-optical characteristics when calculating ocean albedo, particularly in areas experiencing coccolithophore blooms. Future assessments of their role in the Barents and Black seas will apply materials from the Atlas of Bio-Optical Characteristics of the IO RAS [14].

Funding

Hydro-optical modeling was conducted under agreement No. 169–15–2023–002, and the analysis of the results was performed as part of the state assignment of the IO RAS on the topic No. FMWE-2024–0015. The authors would like to thank Corresponding Member of the RAS S.K. Gulev for valuable discussions.

References

1. *Timofeev N.A. Radiation regime of the oceans*. Kiev: Naukova dumka; 1983. 247 p. (in Russian).
2. *Budyko M.I. Heat balance of the earth's surface*. Leningrad: Gidrometeoizdat; 1956. 255 p. (in Russian).
3. *Brooks D.R., Harrison E.F., Minnis P.* et al. Development of algorithms for understanding the temporal and spatial variability of the Earth's radiation balance. *Reviews of Geophysics*. 1986;24(2):422–438. doi:10.1029/RG024i002p00422
4. Gulev S.K., Thorne P.W., Ahn J. et al. Changing state of the climate system. *Climate Change 2021: The Physical Science Basis. Contribution of Working Group I to the Sixth Assessment Report of the Intergovernmental Panel on Climate Change*. Cambridge University Press: 2021. 287–422 p.
5. Bogdanov M.B., Chervyakov M. Yu., Koshel A.A. Ten-year series of global albedo distribution according to the Meteor-M satellite data. *Sovremennye Problemy Distancionnogo Zondirovanija Zemli iz Kosmosa*. 2022;19(2):243–251. doi:10.21046/2070-7401-2022-19-2-243-251
6. Chervyakov M. Yu., Kotuma A.I., Spiryakhina A.A. Atlas of albedo based on measurements of reflected shortwave radiation fluxes obtained using the hydrometeorological satellite Meteor-M No. 1. URL: http://elibrary.sgu.ru/uch_lit/1859.pdf (date of access: 30.03.2024) (in Russian).
7. Rutan D., Rose F., Roman M. et al. Development and assessment of broadband surface albedo from Clouds and the Earth's Radiant Energy System Clouds and Radiation Swath data product. *Journal of Geophysical Research: Atmospheres*. 2009;27:114(D8). doi:10.1029/2008JD010669
8. Donohoe A., Battisti D.S. Atmospheric and surface contributions to planetary albedo. *Journal of Climate*. 2011;24(16):4402–4418. doi:10.1175/2011JCLI3946.1
9. Kopelevich O.V., Sheberstov S.V., Burenkov V.I. et al. Estimation of volumetric absorption of solar radiation in the water column using satellite data. *Fundamental'nye Issledovanija Okeanov i Morej*. M.: Nauka; 2006. 109–126 p. (in Russian).
10. Madec G., Bourdallé-Badie R., Bouttier P.A. et al. *NEMO Ocean engine*. 2017. doi:10.5281/zenodo.6334656
11. Payne R.E. Albedo of the sea surface. *Journal of Atmospheric Sciences*. 1972;29(5):959–70. doi:10.1175/1520–0469(1972)029<0959: AOTSS>2.0.CO;2
12. Jin Z., Charlock T.P., Smith Jr. W.L., Rutledge K. A parameterization of ocean surface albedo. *Geophysical Research Letters*. 2004;31:22. doi:10.1029/2004GL021180
13. Wei J., Ren T., Yang P. et al. An improved ocean surface albedo computational scheme: Structure and Performance. *Journal of Geophysical Research: Oceans*. 2021;126:8. doi:10.1029/2020JC016958
14. Kopelevich O.V., Sahling I.V., Vazyulya S.V. et al. Bio-optical characteristics of the seas washing the shores of the western half of Russia, according to satellite color scanner data from 1998–2017. Moscow: IO RAS; 2018. 140 p. URL: https://optics.ocean.ru/Atlas_2019/8_Monography_2018.pdf (date of access: 30.03.2024) (in Russian).
15. Glukhovets D.I., Sheberstov S.V. Influence of primary hydro-optical characteristics on ocean albedo. *Proceedings of X Anniversary All-Russia Conference «Current problems in optics of natural waters» (ONW'2019)*. Saint-Petersburg: JSC "Izd. "KHIMIZDAT"; 2019. P. 64–69 (in Russian).
16. Plass G.N., Kattawar G.W., Catchings, F.E. Matrix operator theory of radiative transfer. 1: Rayleigh scattering. *Applied Optics*. 1973;12:314–329. doi:10.1364/AO.12.000314
17. Kopelevich O., Sheberstov S., Vazyulya S. Effect of a Coccolithophore Bloom on the Underwater Light Field and the Albedo of the Water Column. *Journal of Marine Science and Engineering*. 2020;8:456. doi:10.3390/jmse8060456
18. Gordon H.R., Castaño D.J. Aerosol analysis with Coastal Zone Color Scanner. A simple method for including multiple scattering effects. *Applied Optics*. 1989;28:1320–1326. doi:10.1364/AO.28.001320
19. HITRAN on the Web https://hitran.iao.ru/home.sim-theory.sp-function (date of access: 30.03.2024).
20. Gordon H.R., Wang M. Surface-roughness considerations for atmospheric correction of ocean color sensors. I: The Rayleigh-scattering component. *Applied Optics*. 1992;32:4247–4260. doi:10.1364/AO.31.004247

21. Mobley C.D., Hedley J.D. Hydrolight 6.0 Ecolight 6.0 Technical Documentation. Numerical Optics Ltd. 2021. Belmont House, 19 West Street Tiverton, EX16 8AA, UK 131 p.
22. Morel A., Antoine D., Gentili B. Bidirectional reflectance of oceanic waters: accounting for Raman emission and varying particle scattering phase function. *Applied Optics*. 2002;41(30):6289–6306. doi:10.1364/AO.41.006289
23. Kopelevich O.V. *Low-parameter model of the optical properties of sea water. Optika Okeana*. M.: Nauka; 1983. Vol. 1, P. 208–234.
24. Segelstein D.J. *The complex refractive index of water. Doctoral dissertation*. University of Missouri-Kansas City: 1981.
25. Stamnes K., Tsay S.-C., Wiscombe W., Jayaweera K. Numerically stable algorithm for discrete-ordinate-method radiative transfer in multiple scattering and emitting layered media. *Applied Optics*. 1988;27:2502–2509. doi:10.1364/AO.27.002502
26. Vazyulya S., Deryagin D., Glukhovets D. et al. Regional Algorithm for Estimating High Coccolithophore Concentration in the Northeastern Part of the Black Sea. *Remote Sensing*. 2023;15(9):2219. doi:10.3390/rs15092219
27. Tyrrel T., Holligan P.M., Mobley C. Optical impacts of oceanic coccolithophore blooms. *Journal Geophysical Research Oceans*. 1999;104:3223–3241. doi:10.1029/1998JC900052
28. Chernokulsky A.V, Mokhov I.I. Intercomparison of Global and Zonal Cloudiness Characteristics from Different Satellite and Ground6Based Data. *Issledovanie Zemli iz Kosmosa*. 2010;3:12–29.
29. Glukhovets D.I., Goldin Yu.A. Surface desalinated layer distribution in the Kara Sea determined by shipboard and satellite data. *Oceanologia*. 2020;62(3):364–373. doi:10.1016/j.oceano.2020.04.002
30. McMahon A., Moore R.D. Influence of turbidity and aeration on the albedo of mountain streams. *Hydrological Processes*. 2017;31(25):4477–4491. doi:10.1002/hyp.11370

Литература

1. *Тимофеев Н.А.* Радиационный режим океанов. Киев: Наукова думка, 1983. 247 с.
2. *Будыко М.И.* Тепловой баланс земной поверхности. Л.: Гидрометеоиздат, 1956. 255 с.
3. *Brooks D.R., Harrison E.F., Minnis P.* et al. Development of algorithms for understanding the temporal and spatial variability of the Earth's radiation balance // Reviews of Geophysics. 1986. Vol. 24, N 2. P. 422–438. doi:10.1029/RG024i002p00422
4. *Gulev S.K., Thorne P.W., Ahn J.* et al. Changing state of the climate system // Climate Change 2021: The Physical Science Basis. Contribution of Working Group I to the Sixth Assessment Report of the Intergovernmental Panel on Climate Change. Cambridge University Press, 2021. P. 287–422.
5. *Богданов М.Б., Червяков М.Ю., Кошель А.А.* Десятилетний ряд глобального распределения альбедо по данным ИСЗ «Метеор-М» // Современные проблемы дистанционного зондирования Земли из космоса. 2022. Т. 19, № 2. С. 243–251. doi:10.21046/2070-7401-2022-19-2-243-251
6. *Червяков М.Ю., Котума А.И., Спиряхина А.А.* Атлас альбедо по данным измерений отраженных потоков коротковолновой радиации, полученных с помощью гидрометеорологического спутника «Метеор-М» № 1. Саратов: Изд-во Сарат. Ун-та, 2017, 57 с. URL: http://elibrary.sgu.ru/uch_lit/1859.pdf (дата обращения: 30.03.2024).
7. *Rutan D., Rose F., Roman M.* et al. Development and assessment of broadband surface albedo from Clouds and the Earth's Radiant Energy System Clouds and Radiation Swath data product // Journal of Geophysical Research: Atmospheres. 2009. Vol. 27. 114(D8). doi:10.1029/2008JD010669
8. *Donohoe A., Battisti D.S.* Atmospheric and surface contributions to planetary albedo // Journal of Climate. 2011. Vol. 24, N 16. P. 4402–4418. doi:10.1175/2011JCLI3946.1
9. *Копелевич О.В., Шеберстов С.В., Буренков В.И.* и др. Оценка объемного поглощения солнечного излучения в водной толще по спутниковым данным // Фундаментальные исследования океанов и морей. М.: Наука, 2006. С. 109–126.
10. *Madec G., Bourdallé-Badie R., Bouttier P.A.* et al. NEMO Ocean engine. 2017. doi:10.5281/zenodo.6334656
11. *Payne R.E.* Albedo of the sea surface // Journal of Atmospheric Sciences. 1972. Vol. 29, N 5. P. 959–970. doi:10.1175/1520-0469(1972)029<0959: AOTSS>2.0.CO;2
12. *Jin Z., Charlock T.P., Smith Jr. W.L., Rutledge K.* A parameterization of ocean surface albedo // Geophysical research letters. 2004. Vol. 31, N 22. doi:10.1029/2004GL021180
13. *Wei J., Ren T., Yang P.* et al. An improved ocean surface albedo computational scheme: Structure and Performance // Journal of Geophysical Research: Oceans. 2021. Vol. 126, N 8. doi:10.1029/2020JC016958
14. *Копелевич О.В., Салинг И.В., Вазюля С.В.* и др. Биооптические характеристики морей, омывающих берега западной половины России, по данным спутниковых сканеров цвета 1998–2017 гг. // Институт океанологии имени П.П. Ширшова РАН. Ответственный редактор д. ф.-м. н. О.В. Копелевич. Москва, 2018. 140 с. URL: https://optics.ocean.ru/Atlas_2019/8_Monography_2018.pdf (дата обращения: 30.03.2024).

15. *Глуховец Д.И., Шеберстов С.В.* Влияние первичных гидрооптических характеристик на альбедо океана // Труды XII Всероссийской конференции с международным участием «Современные проблемы оптики естественных вод», Санкт-Петербург: ИО РАН, 2023. С. 64–69.
16. *Plass G.N., Kattawar G.W., Catchings, F.E.* Matrix operator theory of radiative transfer. 1: Rayleigh scattering // Applied Optics1973. Vol. 12. P. 314–329. doi:10.1364/AO.12.000314
17. *Kopelevich O., Sheberstov S., Vazyulya S.* Effect of a Coccolithophore Bloom on the Underwater Light Field and the Albedo of the Water Column // Journal of Marine Science and Engineering. 2020. Vol. 8. 456. doi:10.3390/jmse8060456
18. *Gordon H.R., Castaño D.J.* Aerosol analysis with Coastal Zone Color Scanner. A simple method for including multiple scattering effects // Applied Optics. 1989. Vol. 28. P. 1320–1326. doi:10.1364/AO.28.001320
19. HITRAN on the Web https://hitran.iao.ru/home.sim-theory.sp-function (дата обращения: 30.03.2024).
20. *Gordon H.R., Wang M.,* Surface-roughness considerations for atmospheric correction of ocean color sensors. I: The Rayleigh-scattering component // Applied Optics. 1992. Vol. 32, P. 4247–4260. doi:10.1364/AO.31.004247
21. *Mobley C.D., Hedley J.D.* Hydrolight 6.0 Ecolight 6.0Technical Documentation. Numerical Optics Ltd. 2021. Belmont House, 19 West Street Tiverton, EX16 8AA, UK 131 p.
22. *Morel A., Antoine D., and Gentili B.,* Bidirectional reflectance of oceanic waters: accounting for Raman emission and varying particle scattering phase function 2002 // Applied Optics. Vol. 41. N 30. P. 6289–6306. doi:10.1364/AO.41.006289
23. *Копелевич О.В.* Малопараметрическая модель оптических свойств морской воды // Оптика океана. М.: Наука, 1983. Т. 1. С. 208–234.
24. *Segelstein D.J.* The complex refractive index of water // Doctoral dissertation, University of Missouri-Kansas City. 1981.
25. *Stamnes K., Tsay S.-C., Wiscombe W., Jayaweera K.* Numerically stable algorithm for discrete-ordinate-method radiative transfer in multiple scattering and emitting layered media // Applied Optics. 1988. Vol. 27. P. 2502–2509. doi:10.1364/AO.27.002502
26. *Vazyulya S., Deryagin D., Glukhovets D. et al.* Regional Algorithm for Estimating High Coccolithophore Concentration in the Northeastern Part of the Black Sea // Remote Sensing. 2023. Vol. 15, N 9. 2219. doi:10.3390/rs15092219
27. Tyrrel T., Holligan P.M., Mobley C. Optical impacts of oceaniccoccolithophore blooms // Journal Geophysical Research Oceans. 1999. V. 104. P. 3223–3241. doi:10.1029/1998JC900052
28. *Чернокульский А.В., Мохов И.И.* Сравнительный анализ характеристик глобальной и зональной облачности по различным спутниковым и наземным наблюдениям // Исследование Земли из космоса. 2010. № 3. С. 12–29.
29. *Glukhovets D.I., Goldin Yu.A.* Surface desalinated layer distribution in the Kara Sea determined by shipboard and satellite data // Oceanologia. 2020. Vol. 62, N 3. P. 364–373. doi:10.1016/j.oceano.2020.04.002
30. *McMahon A., Moore R.D.* Influence of turbidity and aeration on the albedo of mountain streams // Hydrological Processes. 2017. Vol. 31, N 25. P. 4477–4491. doi:10.1002/hyp.11370

About the Authors

GLUKHOVETS, Dmitry I. Cand. Sc. (Phys.-Math.), Leading Researcher, IO RAS; associate professor Moscow Institute of Physics and Technology (National Research University), ORCID: 0000-0001-5641-4227, Scopus AuthorID: 57193736311, SPIN-code (РИНЦ): 6755-2450, e-mail: glukhovets@ocean.ru

SHEBERSTOV, Sergey V. Senior Researcher, IO RAS, ORCID: 0000-0001-8489-2859, WoS ResearcherID: G-1566-2014, Scopus Author ID: 6602841753, SPIN-code (РИНЦ): 6493-8190, e-mail: sheberst@yandex.ru